PulseCounter: An Efficient General-Purpose Algorithm for Detector Signal Pulse-Processing

Dr. Max Fomitchev-Zamilov[1]

[1]Maximus Energy Corporation, founder@maximus.energy

Abstract

We present the PulseCounter algorithm for digital pulse processing suitable for use with a wide variety of alpha, beta, gamma, neutron, x-ray, and other types of radiation detectors. The algorithm includes provisions for baseline correction, exponential decay compensation, and pileup rejection. The PulseCounter algorithm is easy to implement in software and it yields accurate count rates and high resolution spectra.

1. Introduction

Most radiation detectors produce current or voltage pulses corresponding to the detected nuclear particles. Detectors that produce current pulses usually employ charge-sensitive preamplifiers integrating the currents and converting them into voltages [1]. Detectors capable of energy resolution generate pulses with magnitude proportional to the energy of the detected particles. Some detectors such as certain types of scintillators produce pulses with different rise-time depending on the type of particle detected (e.g. gamma or neutron).

Fortunately, it is possible to classify all common detector signals into 4 broad categories:

- **Short unimodal pulses** such as pulses from PMT voltage dividers, SiPM, or proportional counters, Fig. 1; such signals are characterized by rapid rise time ($\lesssim$1 μs) and fast exponential decay (time constant on the order of a few microseconds);

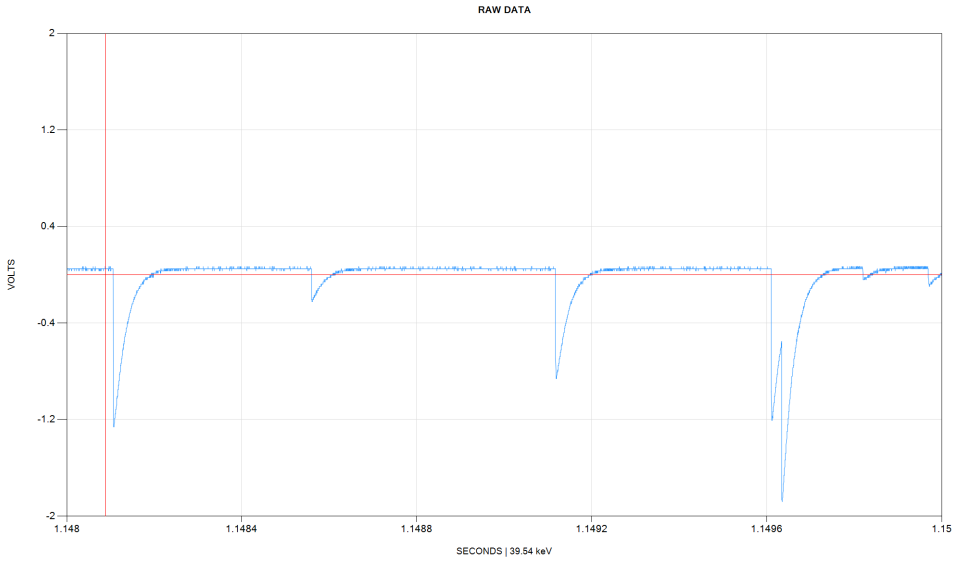

Fig. 1. Short negative unimodal pulses from the anode of a PMT coupled to a NaI(Tl) scintillator.

- **Long step-like pulses** such as the output of a charge sensitive preamplifier, Fig. 2; such signals are characterized by rapid rise time (≲1 μs) and slow exponential decay (time constant on the order of tens of microseconds);

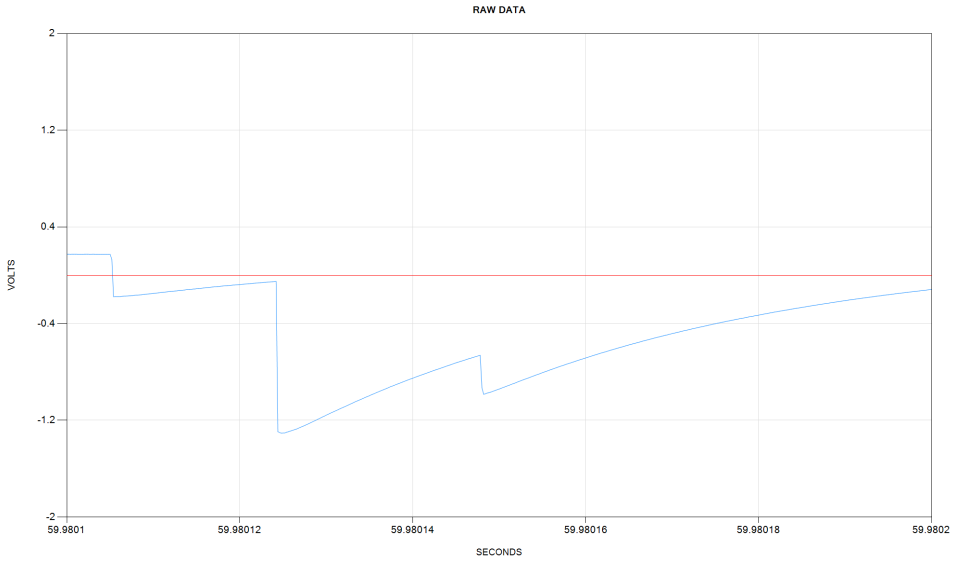

Fig. 2. Long negative step-like pulses from a Canberra resistive feedback charge sensitive preamplifier connected to an HPGe detector.

- **Voltage ramps from reset preamplifiers** typically used with SDD, SiPIN, or Si(Li) detectors, Fig. 3.

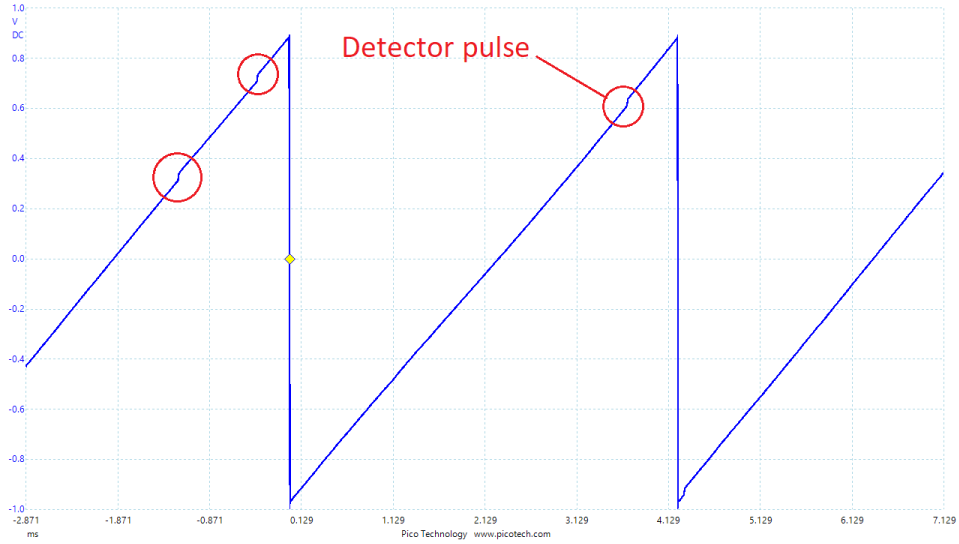

Fig. 3. Voltage ramp from a reset preamplifier connected to a silicon drift detector (SDD); each circled step on the ramp corresponds to an x-ray.

- **Triangular or Gaussian pulses** originating from 3rd party shaping amplifiers or pulse processors, Fig. 4;

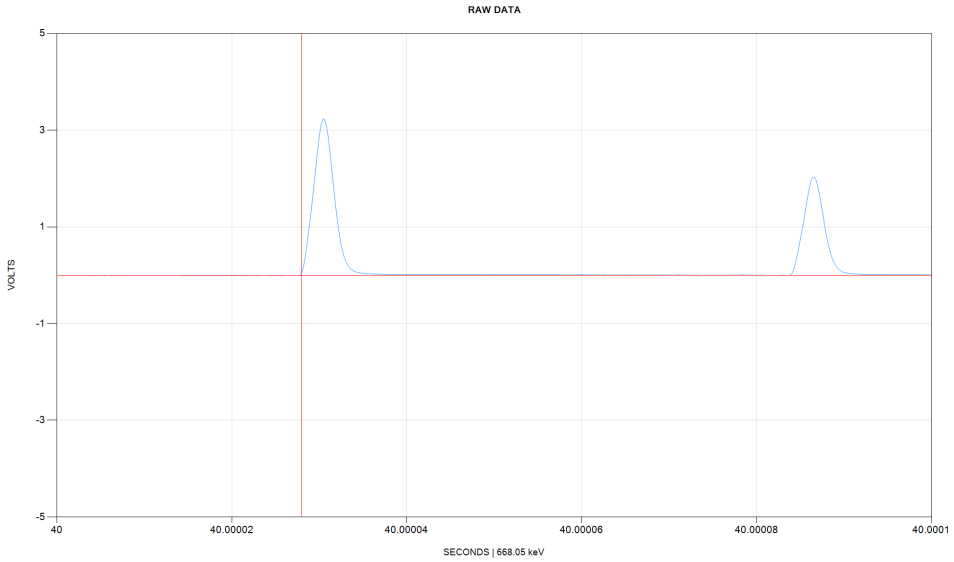

Fig. 4. Positive Gaussian pulses, the output of a Canberra 2026 shaping amplifier.

2. Signal Processing Basics

Detector signals shown on Fig. 1-3 correspond to raw unprocessed signals, which are not suitable for analysis with a multichannel analyzer (MCA) and therefore must be shaped / converted into short unimodal pulses such as Gaussians shown on Fig. 4. Then such shaped pulses can be counted and analyzed.

A typical analog detector signal processing chain is shown on Fig. 5.

Fig. 5. A typical analog detector signal processing chain.

With the advent of digital electronics and digital signal processing (DSP) the analog chain evolved into a diagram shown on Fig. 6.

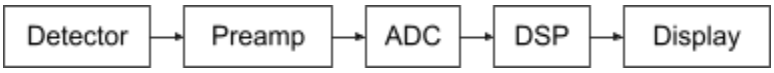

Fig. 6. A typical modern detector signal processing chain.

For the Automated Nuclear Lab (ANL) we have further streamlined the detector signal processing chain and arrived at a configuration shown on Fig. 7 [2].

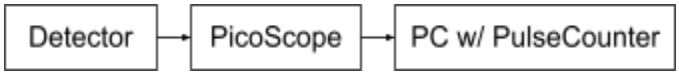

Fig. 7. The ANL detector signal processing chain.

In the latter case the detector signal pulse shaping and analysis is done entirely in software on a PC. The developed PulseCounter software algorithm performs the following tasks:

1) **Pulse shaping:** converts the raw, unprocessed detector signal into a series of unimodal pulses suitable for counting and when appropriate for multi-channel analysis;
2) **Pulse classification:** not all pulses should be counted, some pulses must be rejected based on their undesirable characteristics; for example pulses corresponding to noise or to the wrong particle type (e.g. gammas when counting neutrons) must be rejected;
3) **Multichannel analysis (MCA):** when MCA is appropriate the height of each pulse is measured and a pulse-height spectrum is built;
4) **Pileup rejection:** sometimes closely spaced pulses cannot be accurately resolved / measured and therefore should be excluded from spectrum in order to avoid spectral distortion and prevent the loss of resolution due to spectral peak broadening;
5) **Measurement reporting:** for any given measurement the PulseCounter algorithm produces the total pulse count, the count rate history, the count rate histogram, the pulse rise time histogram, the pulse width histogram, and calculates the count rate mean and standard deviation; additionally the PulseCounter software compiles a list of all detected pulses containing pulse start time, pulse energy and other useful information.

3. Trapezoidal Pulse Shaping

The most commonly used pulse shaping technique is trapezoidal filtering [3]. The idea behind trapezoidal littering is very simple: for every unprocessed sample *S[i]* of a source digital signal compute a processed sample *S'[i]* of the shaped digital signal as a difference between the forward-looking and the backward-looking moving averages:

$$S'[i] = \frac{1}{N}\sum_{j=0}^{N-1} S[i + l + j] - \frac{1}{M}\sum_{j=1}^{M} S[i - j] \qquad (1)$$

The integers *N* and *M* define the length of the moving averages (the length of the filter) and typically *N* = *M*. The integer *l* specifies an optional gap between the forward and the backward-looking moving averages.

If the source signal is a sequence of perfect steps then the resulting shaped signal will be a sequence of perfect triangles (or perfect trapezoids when l > 0), Fig. 8.

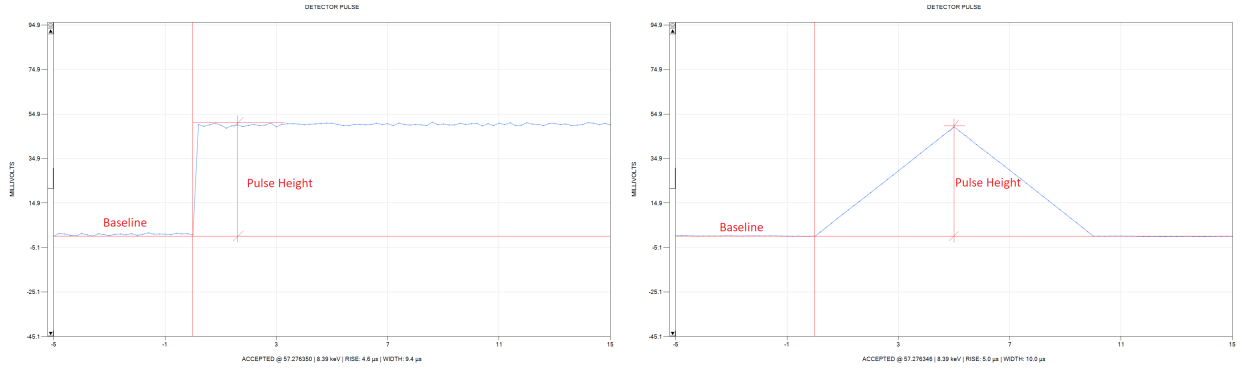

Fig. 8. (Left) A step-like detector signal; (Right) the corresponding triangular shaped pulse.

The height of each triangular (or trapezoidal) pulse of the shaped signal matches exactly the height of each corresponding step of the source signal. The greater is the length of the filter the wider are the resulting triangles (or trapezoids).

The length of the filter is typically chosen to effectively suppress noise, which is always present in any real signal: the greater the noise the longer the trapezoidal filter ought to be in order to yield an accurate estimate of the height of the detector pulse.

When the source signal is completely free from noise a single sample is sufficient to accurately represent each moving average (*N* = *M* = *1*), and the resulting trapezoidal filtering operation transforms into differentiation:

$$S'[i] = S[i + l] - S[i - 1] \qquad (2)$$

Non-zero values of *l* are typically used to compensate for ballistic deficiency [3]: sometimes detector pulses of the same energy can vary slightly in rise time resulting in triangular shaped pulses of slightly variable height thus degrading the energy resolution. To overcome the ballistic deficiency *l* > *0* should be used, yielding slightly imperfect trapezoids with peak heights nevertheless accurately matching the magnitude (energy) of detector pulses.

3.1 Exponential Decay Compensation

In reality however, the raw detector pulses are characterized by both non-zero rise time and exponential decay, Fig. 9 (left). In this case the resulting shaped pulse will be quasi-triangular and it will be followed by the baseline ‘undershoot’, Fig. 9 (right).

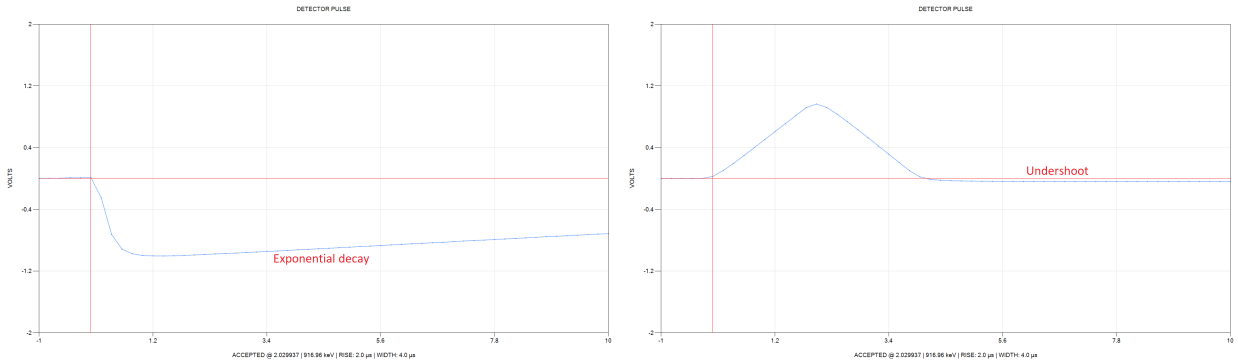

Fig. 9. (Left) a realistic detector signal characterized by non-zero rise time and exponential decay; (Right) the corresponding shaped pulse and the resulting baseline undershoot.

This undershoot introduces a slight baseline drift, which may affect the height of the next shaped pulse. Such baseline drift introduces variability in the shaped pulse height, which ceases to be absolute and instead becomes relative to the drifting baseline. Therefore the baseline drift should be eliminated as it may decrease the energy resolution.

There are three strategies to deal with the baseline drift:

- Increasing the sample rate,
- Exponential decay compensation, and
- Baseline subtraction.

The first strategy involves raising the sampling rate and thus decreasing the apparent magnitude of the exponential decay and therefore making the resulting baseline drift less pronounced.

When increasing the sampling rate is not practical, it is possible to modify the trapezoidal filter to compensate for the exponential decay as follows:

$$S'[i] = \frac{1}{N}\sum_{j=0}^{N-1}\frac{1}{(1-\tau)^j}S[i + l + j] - \frac{1}{M}\sum_{j=1}^{M}S[i - j] \qquad (3)$$

Where τ is the exponential decay time constant of the detector signal:

$$S[i] = S[0]e^{-\tau i} \qquad (4)$$

Because $\tau \ll 1$

$$S[i] \approx S[i - 1]\,(1 - \tau) \qquad (5)$$

We shall call $1 - \tau \lesssim 1$ the adjusted decay constant.

This expression (3) attempts to correct for the exponential decay dividing each sample of the forward-looking moving average by the corresponding power of the adjusted decay constant.

The disadvantage of the exponential decay compensation formula (3) is in its high computational cost. Typically a moving average (and therefore the entire trapezoidal filter operation) can be calculated in just five operations: one addition and one subtraction to update the values of each moving average (4 operations total) and one subtraction to compute the difference between the two moving averages. The same strategy, however, does not work when the exponential compensation is applied because each sample compounding the forward moving average must be weighted differently and therefore for each shaped signal sample *S'[i]* the forward moving average must be calculated from scratch. Nevertheless this technique can be quite effective in eliminating the undershoot and thus enabling the detector signal acquisition at a lower sampling rate.

For slow changing signals or high sampling rates the exponential decay degenerates into linear decay, which introduces a fixed DC offset into the shaped signal baseline. Such decay does not have to be compensated using the equation (3) and instead can be removed via a simple baseline subtraction.

3.2 Pulse Counting and Baseline Subtraction

The shaped pulses are counted by setting a rising edge trigger associated with an arbitrary threshold. In most cases the pulse counting threshold must be chosen to be as low as possible, just above the level of noise. Automatic threshold tuning algorithms typically determine the threshold level by gradually decrementing the threshold while counting pulses. During this process the detector should not be exposed to any radiation sources and the background count rate is expected to be low. The noise level is identified with the value of the threshold coinciding with a sharp increase in the count rate.

Pulses are counted by scanning the shaped signal forward in time with each trigger event counted as a pulse. The height of each encountered shaped pulse is determined by scanning forward and keeping track of the maximum value until the shaped signal returns to the baseline.

The baseline subtraction strategy involves sampling the baseline by computing the average of samples preceding the rising-edge trigger associated with the counting threshold. The proper baseline estimation algorithm, however, is more complicated as the baseline value may be affected by the rising portion of the shaped signal when the threshold level is set too high. Therefore, when using the baseline subtraction one should set the threshold as low as possible, ideally just above the level of noise.

Another pitfall of the baseline estimation approach involves the possibility of running into a preceding shaped pulse when the two pulses happen to occur back to back. Therefore the baseline sampling interval should be short (sometimes just 1 or 2 samples will suffice). For long baseline samples, when scanning backwards one must keep track of the rising-edge trigger associated with the time-reversed threshold crossing indicating the falling slope of the preceding shaped pulse.

It is noteworthy to mention, that corrections due to the baseline drift are generally small and therefore under most conditions affect the resulting pulse height spectrum only in a minor way.

Therefore, the baseline correction is generally important only for very high-resolution spectroscopy using HPGe or silicon-drift detectors. When using these detectors the baseline subtraction may be necessary to achieve the maximum hardware-limited resolution.

3.3 Results

The results of trapezoidal pulse shaping applied to a Bicron 2M2 NaI(Tl) scintillation detector signal captured at 5 MHz / 12 bit and at 10 MHz /12 bit using the PicoScope 4224 digital USB oscilloscope are shown on Fig. 10.

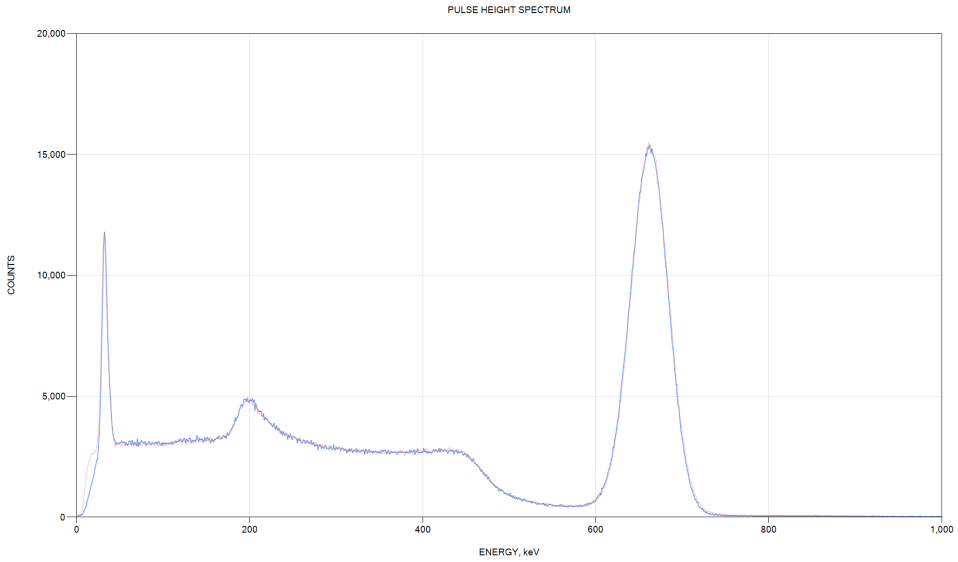

Fig. 10. A ^{137}Cs gamma spectrum obtained using a Bicron 2M2 NaI(Tl) detector; blue spectrum corresponds to the signal captured at 5 MHz / 12 bit, while the red plot corresponds to 10 MHz / 12 bit.

The signal on Fig. 10 was captured using a fairly high count rate of ~46,000 CPM. The spectra obtained using a 10-MHz and 5-MHz signal are nearly identical with no difference in peak width. Trapezoidal pulse shaping with baseline subtraction and exponential decay compensation was used in both cases. Due to the high count rate, without the baseline subtraction the low-energy 32 keV peak cannot be resolved at all. The exponential decay compensation offers only a very minor improvement to the height and width of the 32 keV peak.

Fig. 11 illustrates a ^{137}Cs gamma spectrum obtained using a Canberra HPGe detector. Trapezoidal pulse-shaping of the signal captured at 10 MHz allowed achieving the ultimate hardware resolution of this system of 0.3% FWHM @ 661.7 keV while the signal captured at 5 MHz yielded somewhat lower resolution (Fig. 11 inset). In both cases the exponential decay compensation and the baseline subtraction resulted in an insignificant improvement.

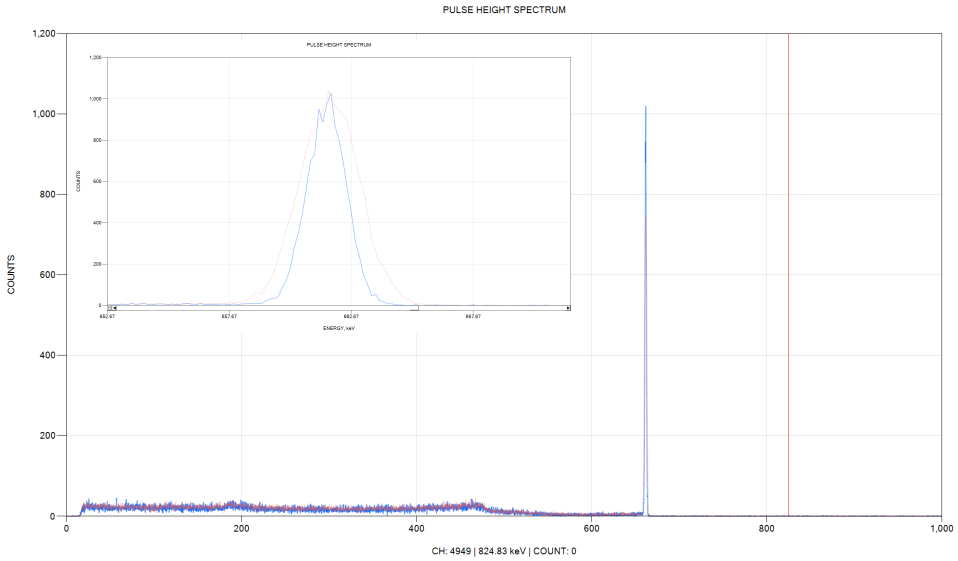

Fig. 11. A ^{137}Cs gamma spectrum obtained using a Canberra HPGe detector; blue spectrum corresponds to the signal captured at 10 MHz / 12 bit, while the red plot corresponds to 5 MHz / 12 bit; (Inset) zooming in on the 661.7 keV peak.

Fig. 12 illustrates a ^{55}Fe x-ray spectrum obtained using an AmpTek SDD detector. Trapezoidal pulse-shaping of the signal captured at 5 MHz / 16-bit using a PicoScope 4262 digital USB oscilloscope allowed achieving the ultimate hardware resolution of the detector of 2.2% FWHM @ 5.9 keV. The exponential decay compensation and the baseline subtraction were not necessary and therefore were turned off.

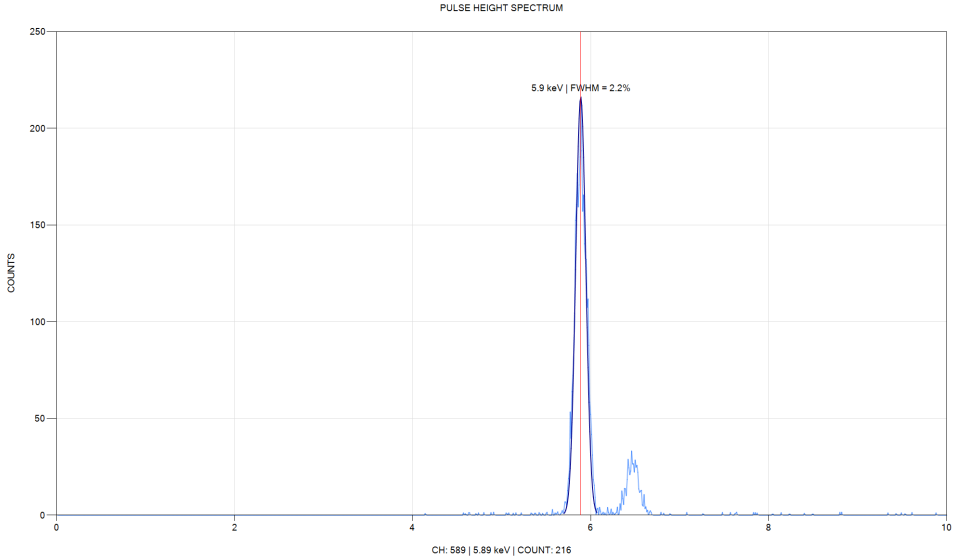

Fig. 12. A ^{55}Fe x-ray spectrum obtained using an AmpTek SDD detector; the signal was captured at 5 MHz / 16 bit.

4. Differential Pulse Shaping

When the noise level is low it may be possible to recover the pulse's energy just from the rising edge of the pulse. For this purpose the raw detector signal can be differentiated and integrated as follows:

$$S'[i] = \sum_{j=0}^{N-1} (S[i + j] - S[i + j - 1]) \quad (6)$$

The advantage of the differential pulse shaping is that it enables very high count rates due to the very narrow width of the resulting shaped pulses. However, the differential pulse shaping does not work well when the detector signal is very noisy, in this case trapezoidal pulse shaping tends to perform better.

Also, the same exponential decay compensation idea applies to the differential pulse shaping: the e differential shaped pulses will exhibit a slight undershoot due to the exponential decay. To remove the undershoot the equation (6) can be rewritten as:

$$S'[i] = \sum_{j=0}^{N-1} (S[i + j] - \frac{1}{1-\tau} S[i + j - 1]) \quad (7)$$

The formula (7) is basically a weighted moving average and therefore unlike the equation (3) it can be computed very efficiently.

When applied to a ^{137}Cs gamma signal captured using a Bicron 2M2 NaI(Tl) detector the equation (7) produced results identical to the ones presented on Fig. 10.

5. Pileup Rejection

Closely spaced pulses in the raw detector signal may result in the overlap of the shaped pulses, causing a pileup - Fig. 13.

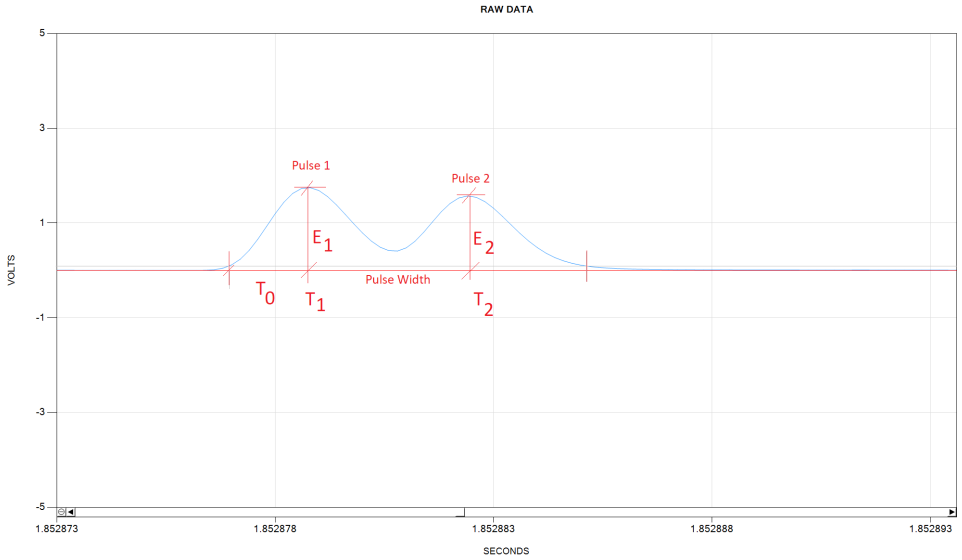

Fig. 13. Pileup of the shaped pulses.

The probability of pile up increases with the increase in the length of the trapezoidal filter as a longer filter results in broader shaped pulses, which would tend to overlap more.

When pileup occurs both piled up pulses should be excluded from the spectrum since the height of both pulses is affected by the overlap. Therefore it is important to recognize the pileup.

The pileup can be recognized by monitoring the secondary differential rising edge trigger condition during the peak height measurement step: if the second trigger event occurs prior to the shaped signal returning to the baseline then we have a pileup.

Additionally, the pileup can be detected by examining the pulse width and the rise time histogram of the shaped pulses. Piled up pulses would tend to have larger width and longer rise time and therefore can be easily identified on the histogram, Fig. 14.

Also, it is possible to correct for the two-pulse pileup by computing the corrections to the heights of the piled up pulses as follows:

$$E_2' = (E_2 - E_1 \gamma) / (1 - \gamma^2) \quad (8)$$

$$E_1' = E_1 - E_2' \gamma \quad (9)$$

Where E_1' and E_2' are the corrected (true) pulse magnitudes, E_1 and E_2 are the apparent pulse magnitudes, and γ is defined as:

$$\gamma = (T_0 - T_2 + T_1) / T_0 \quad (10)$$

Where T_0 is the filter length in time units, $T_2 - T_1$ is the time interval between the peaks of the two piled up pulses.

This correction recovers the original pulse heights of the two overlapping pulses and thus makes their exclusion from the spectrum unnecessary.

The piled up pulses that are spaced so closely together that they merge into a single shaped pulse can be excluded on the basis of the anomalously large pulse width or rise time. Fig. 14 shows the rise time and the pulse width histograms of the shaped pulses used to construct the spectrum on Fig. 10; the rise time and the pulse width ranges indicating pileup are highlighted in gray.

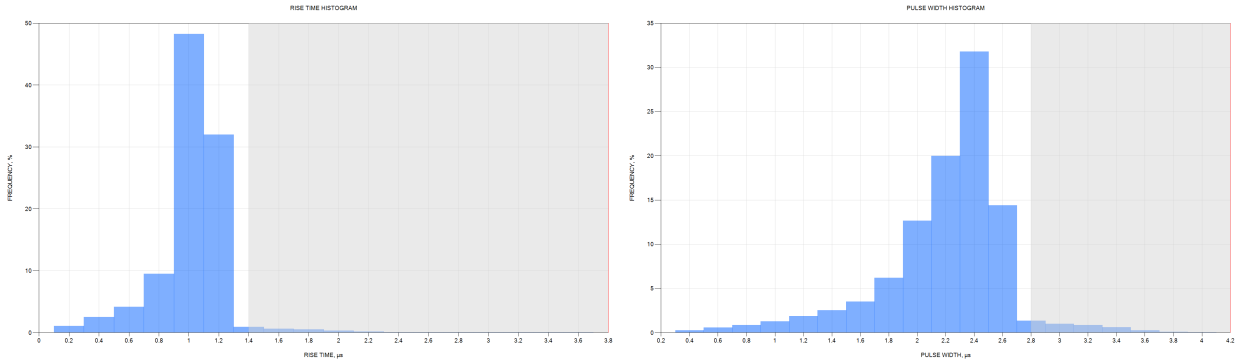

Fig. 14. (Left) the rise time histogram, and (Right) the pulse width histogram of the shaped pulses used to construct the spectrum on Fig. 10; the grayed out areas mark the ranges used to identify the piled up pulses.

Fig. 15. illustrates the effect of the exclusion of the piled up pulses identified by the histograms shown on Fig. 14 from the logarithmic ^{137}Cs spectrum, a significant reduction of artificial high energy counts is evident.

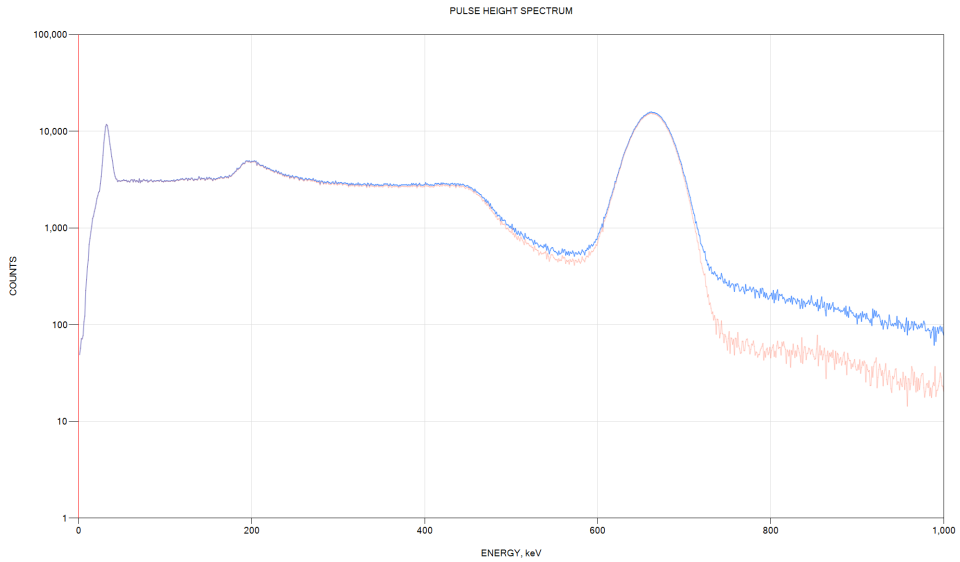

Fig. 15. The logarithmic ^{137}Cs spectrum illustrating the effect of the exclusion of the piled up shaped pulses; the original spectrum is shown in blue; the spectrum after the exclusion of the piled up pulses is shown in red.

Conclusion

We have described the PulseCounter, a general-purpose algorithm for detector signal pulse-processing. The algorithm is suitable for use with a wide variety of nuclear instruments including alpha, beta, gamma, neutron, and x-ray detectors and counters. The algorithm includes provisions for baseline correction, exponential decay compensation, and pileup rejection. Using the PulseCounter algorithm we were able to obtain high-resolution spectra for scintillation, HPGe and silicon drift detectors (SDD). We have shown that for gamma scintillators it is sufficient to capture the detector signal at 5 MHz / 12 bit; for HPGe systems 10 MHz / 12 bit is best; and for SDD 5 MHz / 16 bit is necessary. In all cases we used Pico Technology PicoScope digital USB oscilloscopes to acquire the detector signals. The pulse processing was performed in real time using PulseCounter Pro Windows 10 software [4].

References

1. Charge sensitive preamplifiers explained, Cremat Inc., https://www.cremat.com/why-use-csps/ (2023)
2. Max Fomitchev-Zamilov, Automated Nuclear Lab and PulseCounter Pro: The Tools for Rapid Nuclear Experimentation, https://maximus.energy/wp-content/uploads/2023/10/Antuomated-Nuclear-Lab.pdf (2023)
3. V. Radeka, Trapezoidal filtering of signals from large germanium detectors at high rates, Nuclear Instruments and Methods, Volume 99, Issue 3 (1972)
4. Max I. Fomitchev-Zamilov, Automated Nuclear Lab and PulseCounter Pro Manual, https://maximus.energy/wp-content/uploads/2023/07/PulseCounter-Pro-Manual.pdf (2023)